JOURNAL OF GEOPHYSICAL RESEARCH, VOL. 94, NO. A5, PAGES 5350-5366, MAY 1, 1989

Radar and Optical Measurements of Ionospheric Processes Associated With Intense Subauroral Electric Fields

JAMES F. PROVIDAKES, MICHAEL C. KELLEY, AND WESLEY E. SWARTZ

School of Electrical Engineering, Upson Hall, Cornell University, Ithaca, New York

MICHAEL MENDILLO

Department of Astronomy, Boston University, Boston, Massachusetts

JOHN M. HOLT

Haystack Observatory, Massachusetts Institute of Technology, Westford

Observations of very large poleward directed electric fields were obtained with a clustered set of instrumentation that included the Millstone Hill incoherent scatter radar, the Boston University Mobile Ionospheric Observatory, and the HILAT and Defense Meteorological Satellite Program (DMSP) F6 and F7 satellites. In this paper we concentrate on data from the Millstone Hill incoherent scatter radar which was operated on selected evenings in a rapid azimuthal scan, centered on magnetic west. The mode was designed with the express purpose of measuring line-of-sight drift velocity and electron density as a function of latitude during events with large localized electric fields. During this same period, the Defense Nuclear Agency HILAT satellite made northern hemisphere measurements every 100 min of ion drift, density, and field-aligned currents across the equatorial boundary of the auroral oval. A detailed study of optical data in this region is provided in a companion paper. On the evenings of April 20 and 21, 1985, during an intense magnetic storm ($K_p > 8^+$), large ionospheric electric fields ($E > 80$ mV/m) were detected along the edge of the auroral oval with the Millstone Hill incoherent scatter radar. These constitute the first definitive incoherent scatter observations of this phenomenon. An L shell-aligned (zero order) deep trough in electron density was colocated with these large electric fields at L shells as low as $L = 2.8$. These data indicate that the trough develops much more quickly than present theories predict, at least near the F peak. We also report elevated ion and electron temperatures in the trough and conjecture that these may contribute to the rapid decay. We also show that the associated field-aligned currents are very weak, as predicted by Banks and Yasuhara (1978) but that it is the F region structure which dominates the conductivity gradient rather than the E region emphasized by the earlier work. We also discuss the data set in light of competing theories for the production of large electric fields and for undulations of the edge of the diffuse aurora. In particular we discuss the importance of large radial ion temperature gradients indicated by the DMSP data we present.

INTRODUCTION

In situ observations of large electric fields in the premidnight, high-latitude ionosphere were first published by *Smiddy et al.* [1977] using S3-2 satellite data, and subsequently by *Maynard et al.* [1978], *Spiro et al.* [1979], and *Rich et al.* [1980] using satellite-borne electric field detectors or particle drift meters. These observations have shown that very large localized poleward directed electric fields form along the edge of the auroral oval with strengths as high as 350 mV/m perpendicular to the magnetic field at altitudes around 1300 km, corresponding to westward directed flows of up to 10 km/s. *Maynard et al.* [1980] have also detected large localized electric fields directed radially outward in the equatorial plane near $L = 4$. *Labelle et al.* [1988] have reported a localized intense plasma flow region at 1500 local time at similar L values. To our knowledge no examples of coincident large localized flow and large electric fields have been reported at magnetospheric altitudes.

All of the above observations have been based on satellite data which typically consist of a few minutes of data spaced hours or days apart. In mid-April 1985, a multi-instrumented experiment was conducted at the Millstone Hill incoherent scatter radar facility in Westford, Massachusetts, for the purpose of obtaining the first continuous and extensive ground-based radar and optical measurements of these large electric fields and their effects on the ionospheric and magnetospheric plasma. HILAT and Defense Meteorological Satellite Program (DMSP) satellite data were also obtained during this period, which provided the first simultaneous measurements of these large localized electric fields by both satellite and ground-based incoherent scatter radar. This paper and the companion paper by *Mendillo et al.* [this issue] describe the radar and optical measurements and the geophysical conditions leading to the large fields, and provide some insights into the various mechanisms involved. These data provide information on magnetosphere-ionosphere

Paper number 88JA03874.
0148-0227/89/88JA-03874$05.00

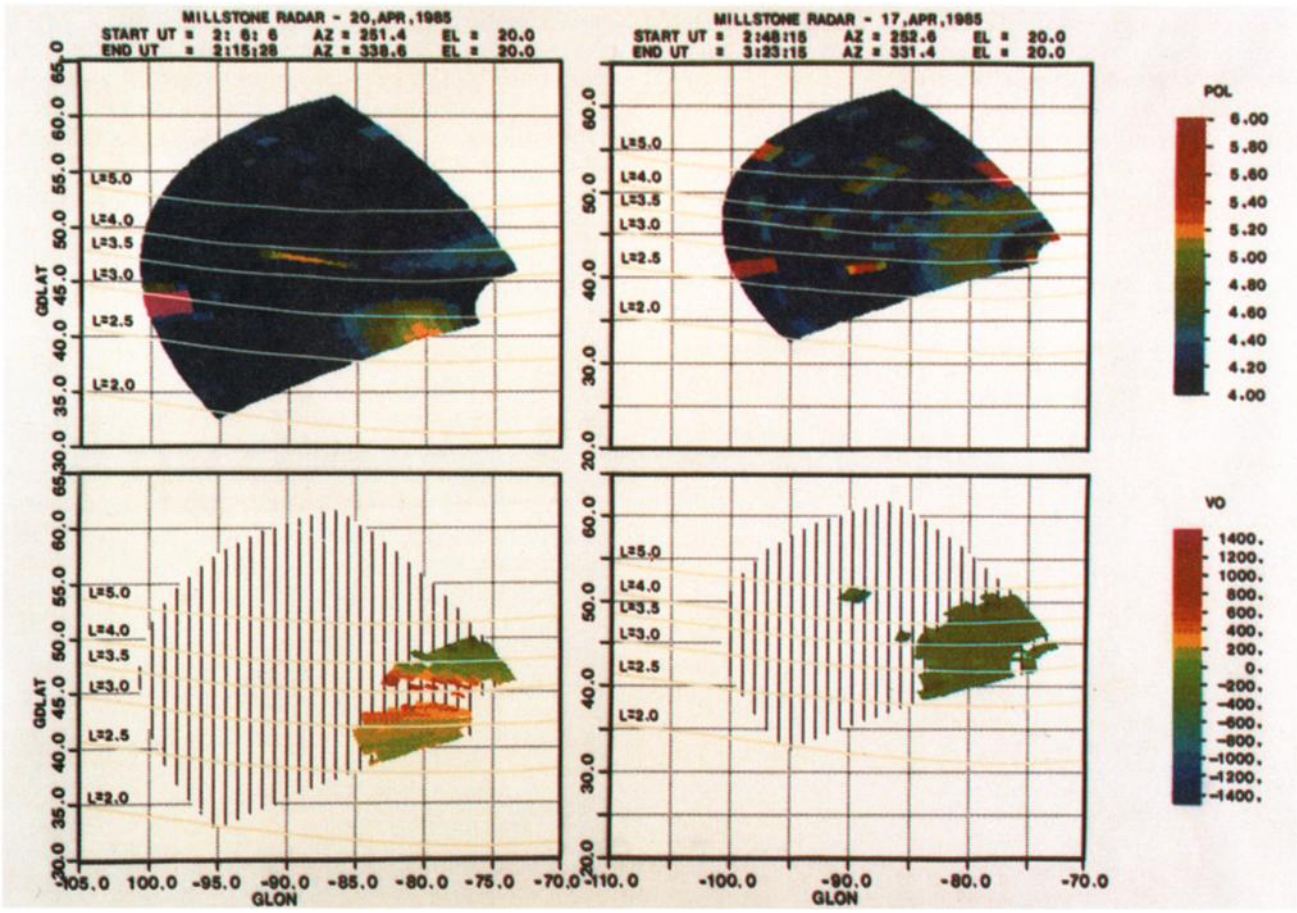

Plate 1a Plate 1b

Plate 1. (top) Electron density profile scan plotted on a logarithmic scale versus geographic coordinates during active conditions. (bottom) Line-of-sight ion velocity drifts (meters per second). Red indicates flow toward the radar, and blue is away. L shell contours are superposed on all of the figures. The local time (LT) was 5 hours behind universal time (UT). The magnetic local time for the trough center shown in Plate 1*a* at the altitude of 309 km (45° latitude and 80° W longitude) was approximately 2040 MLT.

coupling in a very dynamic portion of the inner magnetosphere as well as on an apparent magnetospheric instability in this region.

Data Presentation

Due to the extremely localized nature of the phenomena, a special radar data-taking scanning sequence at Millstone Hill was implemented. This mode (subsequently called the Cornell mode) employed a 1-ms pulse at a fixed elevation of 20°. The radar scanned in a westerly direction (azimuth of 252°-337°) sampling ranges from 300 km to 3000 km (100 km to 1500 km in altitude) with an integration time of 30 s for every 5° of azimuth on April 21, and with an integration time of 15 s for every 2.5° on April 20. This mode was dedicated to studying the small-scale flow and density-depleted structures at the edge of the diffuse aurora. During these two periods, localized regions of large westward line-of-sight velocities were often observed that exceeded 1500 m/s. Coincident with these large velocities were distinct localized plasma depletion regions or troughs. Radar data are available for other times during the 4-day period using a low-elevation 300° azimuth scanning mode that emphasized measurements further to the north to complement data from the Active Magnetospheric Particle Tracer Explorerer (AMPTE) satellite (Foster, personal communication, 1987).

Plate 1*a* shows the electron density and the ion drift velocity along the radar line of sight from the azimuthal radar scans taken on April 20 in the Cornell mode. We have chosen this particular April 20 scan since it coincided with a nearby HILAT satellite pass. There is considerable structure in the electron density profile, and a deep electron density trough can be clearly seen at an L shell of 3.5. Along the boundary of this trough, large westward plasma drifts (> 1500 m/s) were detected, while in the center of the trough, the radar signal to noise ratio becomes too low for the automated display program to yield reliable velocities. Special processing must be used in this region. This figure for a magnetically disturbed day can be contrasted with Plate 1*b* for the quiet day of April 17 (Kp less than 2^+) which had a typical mid-latitude F region peak in electron density and ion drift velocities less than 20 m/s.

Another interesting feature that can be seen in Plate 1*a* is a region of strong signal power located at the poleward and equatorward edges of the electron density trough. Similar examples of enhanced signal power often occurred near the trough in many of the April 20-21 radar scans. Preliminary examination of the spectra for these regions of enhanced signal power shows these spectra to have unusual shapes

that cannot be explained with the basic incoherent scatter theory. These unusual spectra have shapes that are similar to spectra observed by coherent radars.

Figure 2 in the companion paper (*Mendillo et al.*, this issue) shows the *Kp* and *Dst* indices for the 4-day period covering the times of all the measurements reported here. The well-defined magnetic storm evidenced in the figure at times produced visible aurora well to the south of the Boston area. Figure 1 in this paper shows superimposed magnetograms from the San Juan, Puerto Rico, and Fredericksburg, Virginia, stations together with a separate panel for College, Alaska, in which the magnetic field *H* components are plotted for April 19-21, 1985. The horizontal bars on the magnetograms indicate the periods when the Millstone Hill radar operated in the Cornell mode, and arrows mark passes by the HILAT and by two DMSP satellites (F6 and F7) which have been used in this study. Periods when optical data were obtained are indicated in Figure 2 of *Mendillo et al.* [this issue]. At the peak of the magnetic storm (April 21), a *Kp* index of 8^+ was registered. Our Figure 1 shows a good correlation between the San Juan and Fredericksburg magnetometer stations until 2200 UT on April 20. At 2200 UT, the San Juan magnetogram trace went off scale (negatively) for several hours and stayed negative even after returning to on-scale values, all in response to the developing magnetic storm. The Fredericksburg signal, however, changed sign at 0200 UT on April 21, suggesting that Fredericksburg became an auroral zone station for a while, responding to ionospheric currents in the eastward electrojet rather than to the magnetospheric ring current. This implies that the auroral oval had moved to very low *L* shells which is confirmed by the optical measurements of *Mendillo et al.* [this issue].

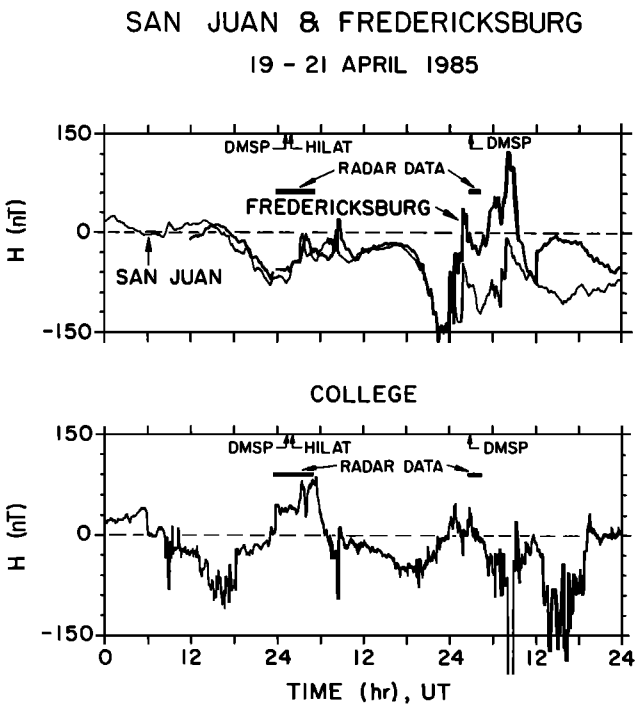

Fig. 1. The magnetic field *H* components from the San Juan (18° N, 66° W), Fredericksburg (39° N, 77° W), and College (65° N, 147° W) stations for April 19-21, 1985. The times of radar observations and the satellite passes are marked.

In this section we first look at the short period of data which was obtained in the Cornell mode during the period of maximum activity (0300 UT on April 21). Although brief in time, this period is important since it provided the only simultaneous optical data. However, since the earlier data set of April 20 is longer and is better centered on the observing grid (because the auroral oval was in a more normal position), this data set is more conducive to detailed study and is therefore emphasized somewhat more than the data obtained on April 21. Unfortunately, the April 20 day was cloudy, and no optical data are available.

April 21, 1985

On April 21, a 45-min period of the Millstone Hill radar operating time was allocated to the Cornell mode. Five azimuthal scans were obtained in this time. Figure 2 shows the first scan on April 21. The electron density measured by the Millstone Hill radar is plotted in a geomagnetic coordinate system. We chose geomagnetic coordinates since the density trough and large electric fields were, to zero order, *L* shell aligned. On this day the *Kp* index exceeded 8^+, and the electron density trough was very far equatorward (*L* shell ≈ 2.5). It should be noted that the changes in plasma density in this display are due both to the variation of density with altitude as well as its variation with latitude. Nevertheless, it is clear that a deep trough is present at the equatorward edge of the scan.

The corresponding optical image is presented in the upper left hand position of Plate 2. In this figure, the four images correspond to the 45-min period encompassed by the radar time in the Cornell mode. The radar intersection point at 300 km altitude is superposed on the upper left-hand image. It is clear that the increase in plasma density on the trough poleward edge (superposed on the same image) is colocated with the increase in the diffuse auroral emissions. In the companion paper [*Mendillo et al.*, this issue], a quantitative comparison is presented which shows that the light emissions at 6300 Å must be associated with impact ionization rather than merely emissions of photons due to the recombination process in a region of enhanced plasma density. This is an important result since it implies that the ionospheric plasma is organized by magnetospheric processes imposed from above.

At the largest scales, the optical emissions are zero order *L* shell aligned. Smaller-scale features, with wavelengths of the order of 200 km in the zonal direction, display north-south contour displacements of several tenths of an *L* shell. At ionospheric heights, one-tenth of an *L* shell value corresponds to about 50 km. As many as three undulations can be seen in the edge of the diffuse aurora. We believe that these data are the first confirmation by Earth-based observations of the results of *Lui et al.* [1982], who reported from DMSP data that the equatorward edge of the diffuse aurora often displays undulations of this type. Satellite observations of longitudinal structure in the poleward edge of the trough region have been reported by *Rodger et al.* [1986], who also showed that the trough poleward edge was dependent upon the equatorward position of a 1-keV electron precipitation boundary (diffuse aurora).

Although not definitive, comparison of these four images shows little evidence for a phase propagation. This is

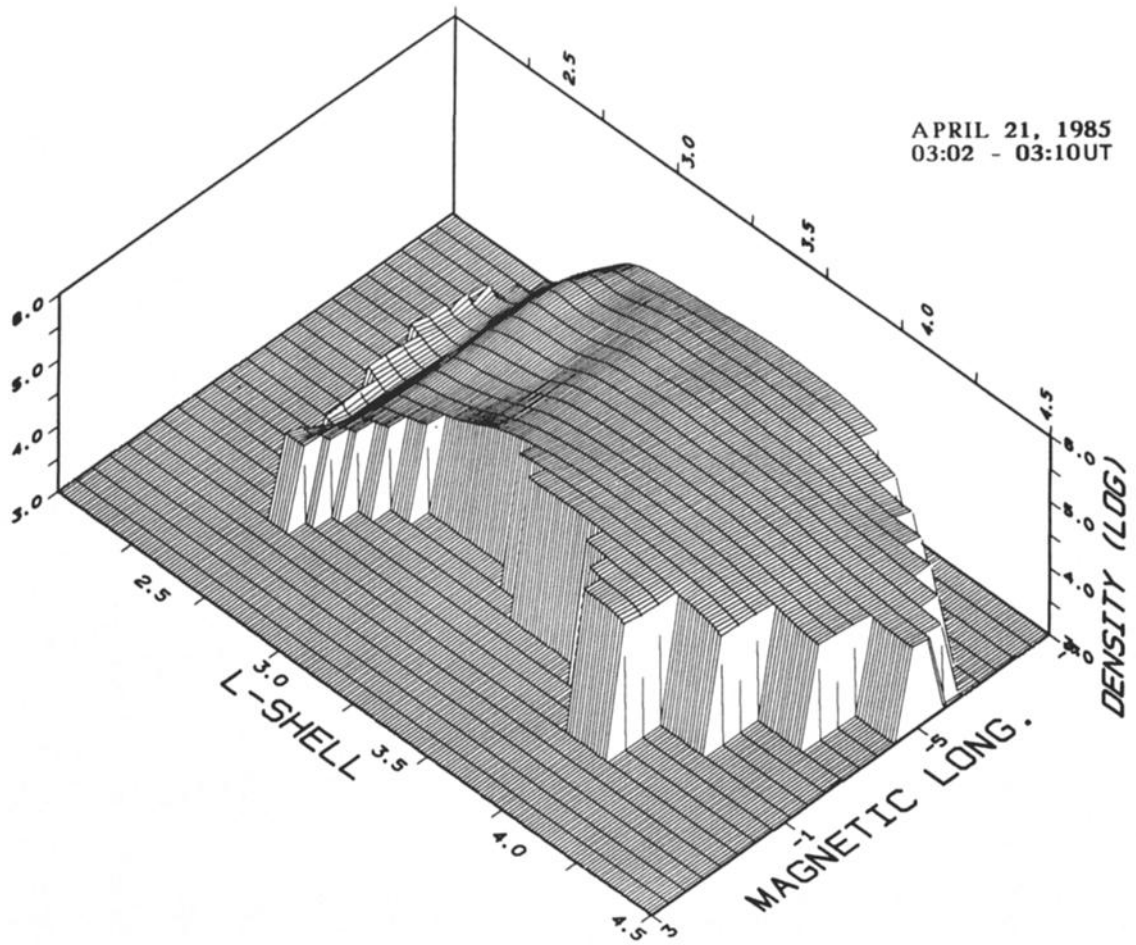

Fig. 2. Electron density scan plotted on a logarithmic scale versus magnetic coordinates. The plot covers an altitude of 187-488 km.

confirmed by a more detailed study in the companion paper [*Mendillo et al.*, this issue] in which the undulations are described as standing wave patterns which grow or decay in amplitude but which do not seem to propagate zonally. We return to this point in the discussion section.

Figure 3*a* is a plot of the electric field and plasma density measured during the same scan shown in Figure 2 as a function of distance from the trough at a fixed altitude of 309 km (see the appendix for discussion of the calculation of the electric fields from the line-of-sight velocities). In this plot, 100 mV/m corresponds to 2000 m/s in the westward direction. Figure 3*b* shows the corresponding electron and ion temperatures measured by the Millstone Hill radar. Whenever there are unresolved velocity shears or other unusual plasma phenomena, the standard radar data analysis programs can overestimate the ion temperature while underestimating the electron temperature, a point that is addressed by *Swartz et al.* [1988] with reference to the same data set under discussion here. We have dashed the ion temperature curve in those regions where these effects may be present. As discussed by *Swartz et al.* [1988], we believe that the velocity shear effect is the most important process in determining the shape of the data set presented here and that the ion temperature is not as high as indicated by the dashed curve.

In Figures 3*a* and 3*b* we use an L shell-aligned trough coordinate system with the center of the trough chosen from the data to be at an L shell of 2.5. For the purpose of determining the trough system, we make the zero-order assumption that the trough structure is independent of magnetic longitude. This allows us to use all the data in a given scan to characterize the latitudinal character of the trough. The data are then plotted versus L shell. For comparison purposes a relative invariant latitude scale is shown at the top of Figures 3*a* and 3*b* with 0° corresponding to the origin of our trough coordinates. Roughly speaking an incremental change of 0.2° invariant latitude is 24 km at the F region altitude of 309 km.

In deciding the origin of the trough coordinate system to use, one has to decide whether to base it on the variations of the measured plasma density or the electric field profiles. The shape of the plasma density profile in the ionosphere will be different at various altitudes because of different chemical and dynamical processes that occur at different altitudes. However, the electric fields measured should be very similar in form and magnitude at all altitudes along the same magnetic field line. Since the electric fields at various altitudes are similar, we chose the electric field profile measured at a constant altitude of 309 km because of the good signal to noise ratio at that height and the absence of coherent echo contamination from electrojet turbulence that was present in some of the radar scans for

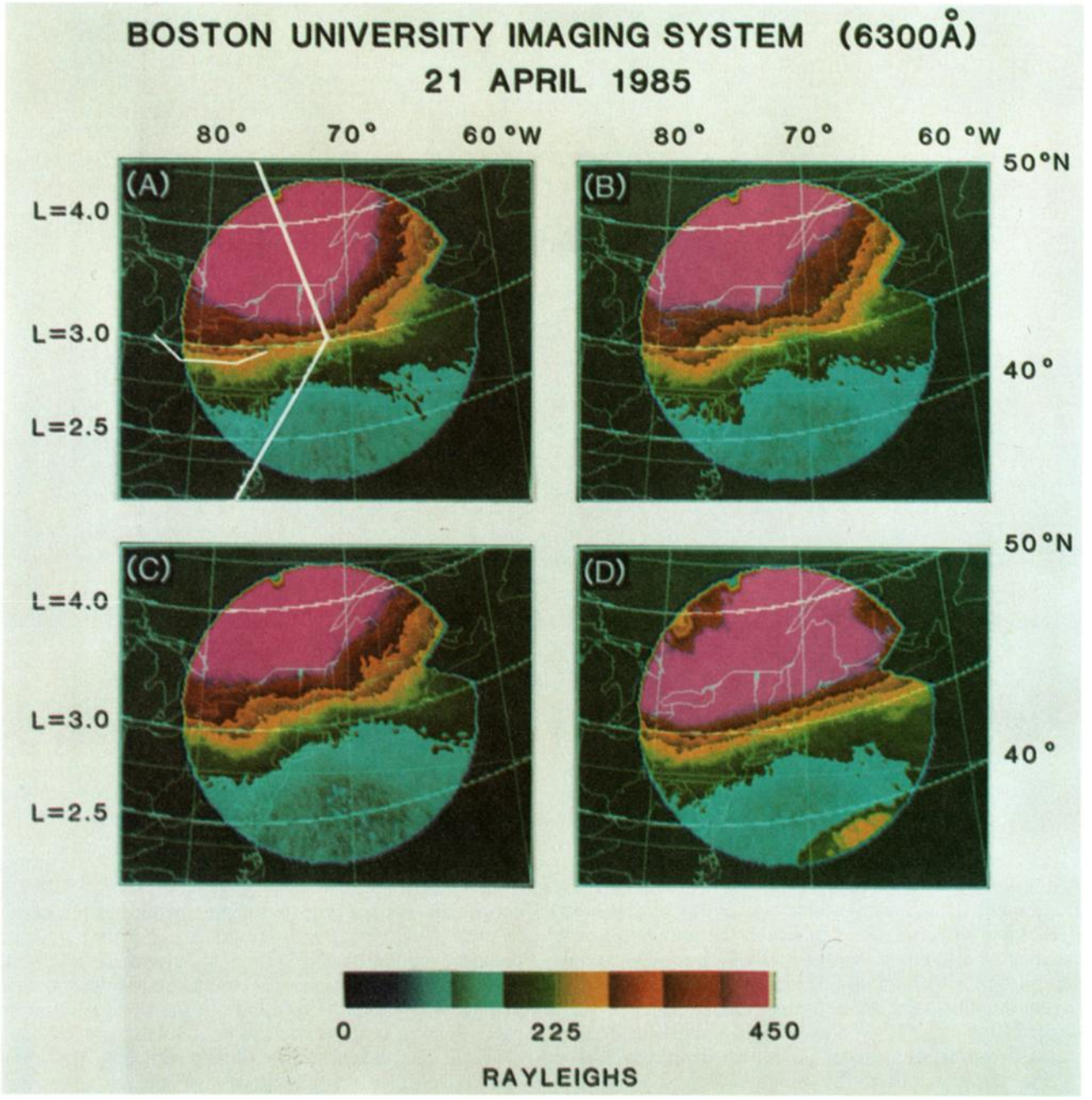

Plate 2. Four optical images that correspond to a 45-min period encompassed by the radar scan time in the Cornell mode on April 21, 1985: (*a*) 0305 UT, (*b*) 0313 UT, (*c*) 0320 UT, and (*d*) 0343 UT. Integration time was 30 s for each image. The north and south boundaries of the radar scan and the position of the trough's poleward edge are superimposed on Plate 2*a*.

the lower altitudes (less than 200 km). However, for those periods during the radar observations where we were unsuccessful in calculating the electric fields within the deepest portion of the trough we used the measured plasma density minimum as our criterion for the determination of the trough center.

In Plate 1*a* and Figure 3, one notices data gaps within the center of the trough region. Although we succeeded in seeing large electric fields and high electron and ion temperatures on the edges of the plasma trough region, a poor signal to noise ratio within the trough region prevented the radar from making any useful measurements in the heart of the trough. Since the dynamical processes had time scales of the order of only a few minutes, we could not use a longer integration time without sacrificing important details of the spatial structuring of the density trough region. We believe that the electric field was most likely larger in the central portion of the trough given the satellite results referenced above.

Figures 4*a* and 4*b* show the precipitating ion and electron fluxes obtained from the DMSP F6 satellite a few minutes before the first Cornell scan. The data are plotted in the same L shell trough coordinate system used in Figure 3. One can clearly see that the auroral precipitation extended

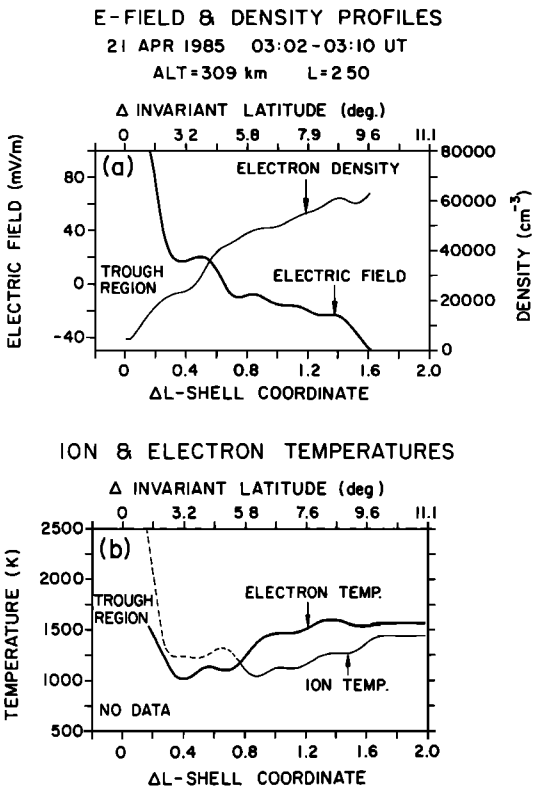

Fig. 3. (*a*) Radar-measured electric field and plasma density profiles at an altitude of 309 km. (*b*) Corresponding electron and ion temperature profiles. The electron and ion temperatures have an accuracy of better than 5% for $\Delta L > 0.7$ and 10% for $\Delta L < 0.7$. Both figures use an ΔL shell (invariant latitude) aligned electron density trough coordinate system.

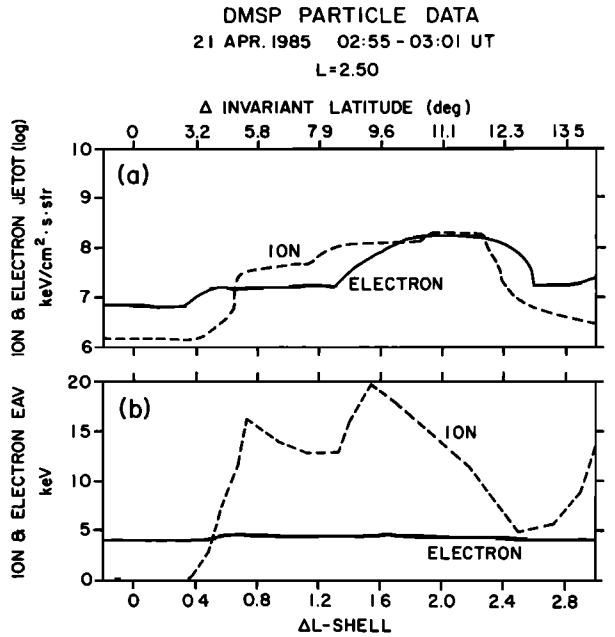

Fig. 4. (*a*) Total ion and electron energy flux. (*b*) Electron and ion average energy. Both figures use the same L shell (invariant latitude) trough coordinate system centered at $L = 2.50$. A significant change in the ion total flux and average energy occurred between $\Delta L = 0.40$ and 0.65. There was no clear change in the electron average energies although a significant change in the electron flux occurred between $\Delta L = 1.30$ and 1.70.

to very low latitudes. Although the plot covers more distance than Figure 3, the L shell spacing is identical and can be overlaid for reference. The satellite measurements were nearly simul-taneous with the radar data but shifted roughly 3 hours in local time (≈1800 MLT). Given this large spatial separation it is remarkable that the poleward edge of the plasma density trough near Millstone Hill agrees so well with the ion and electron precipitation boundaries. Notice that the ion precipitation ends at about $\Delta L = +0.6$ which is equatorward of the electron precipitation boundary which ends at $\Delta L = +1.3$. This is typical of this local time sector [*Gussenhoven et al.*, 1987] and indicates that the ions at the edge of the magnetospheric ring current have moved farther earthward than the electrons.

April 20, 1985

Figure 5 is an expanded plot of the San Juan magnetogram which focuses on the time when the Millstone Hill radar was being operated in the Cornell mode on April 20, 1985. The L value of the plasma density trough is plotted in the same figure versus time. We did not include any partial radar scans in the generation of the curve that shows the location of the trough. At the beginning of the day (in universal time), a plasma density trough developed at an L shell of 3.8. The position of the trough moved equatorward (L shell ≈ 3.4 at 0130 UT) during the next hour while the *Dst* index and San Juan H component slightly decreased, indicating a steady or slightly increasing ring current intensity. In Figures 6*a* and 6*b* the density and velocity profiles are presented as a function of time. Notice that the large localized westward velocity observed around 0030 UT preceded the development of a deep plasma density trough. The H component at San Juan and the *Dst* index both recover to the baseline at about 0120 UT. Simultaneously the radar measured a decrease in the magnitude of the large westward line-of-sight velocities and a slight poleward shift in the trough location. The depletion in the plasma density trough became more broad and the line-of-sight velocities decreased, until finally at 0250 UT it was not possible to

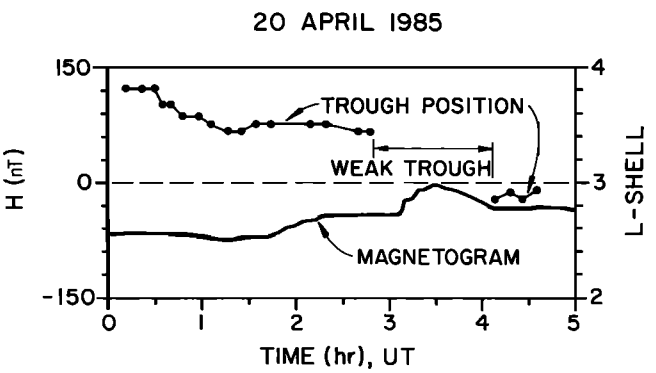

Fig. 5. Magnetometer data from the San Juan station for the H component plotted versus universal time while the Millstone Hill radar operated in the Cornell mode on April 20, 1985. The L value of the trough minimum is also plotted.

determine at what L shell the trough was located. Then at 0330 UT, magnetic activity sharply increased as indicated by an intensification of the ring current detected at San Juan and of the eastward electrojet detected at College, Alaska (see Figure 1). The radar again measured large westward drift velocities which were followed by development of a plasma density trough. This structure developed at a much lower L shell value (≈2.8). It is interesting to note that the negative $\partial B/\partial t$ for this period was greater than the previous one, indicating a possible relationship between plasma trough position and the value of $\partial B/\partial t$.

Figure 7 shows the plasma density trough in more detail at 0210 UT, which was near the end of the first period of trough observation. In the geomagnetic coordinate system the density trough is clearly seen to be L shell aligned. In contrast to Figure 2, during this less active day the radar could be used to observe regions both poleward and equatorward of the density trough. Equatorward of the trough, the smooth high-density plasma is a remnant of the solar-produced plasma from the previous day. Figure 8 shows a series of plasma density profiles separated by units of 0.18 in L shell parameter obtained from this same data set. The density profile equatorward of the trough region exhibits features typical of a quiet day. In the heart of the trough there is a distinct flattening of the F region to the extent that almost no peak occurs. A peak reappears in the region poleward of the trough, but it is much lower in altitude and density. Also, the plasma scale height above this peak is approximately 3 times larger in and just poleward of the trough than it is either to the south or to the north. This indicates an increased electron temperature. In one of the profiles (L = -0.18) we have been able to determine the E region density from measurements made by the Millstone Hill radar. The data show the E region to be less than or equal to a typical nighttime E region profile. Figures 9*a* and 9*b* show the latitudinal variation in the plasma density and the electric fields (derived from line-of-sight radar observations) in the trough coordinate system for the same April 20 scan. The data gap in the temperatures occurred as the radar scanned near the center of the trough region. The Millstone Hill incoherent scatter data base programs were unsuccessful in calculating the temperatures and velocities in this region. A preliminary analysis of the spectrum in that region suggests that the majority of the data were thrown out because of either poor signal to noise ratio or distortion from the predicted model of the incoherent scatter spectrum. Although some of the spectra appear to be slightly asymmetrical, those spectra within the trough region exhibit a very large Doppler shift (> 1000 m/s) which allows one to at least determine the ion velocities which are plotted in Figure 9*a*. In the appendix we discuss the program used to derive the line-of-sight velocities in these regions where the Millstone Hill maximum likelihood estimate techniques failed. The region of maximum electric field strength (> 80 mV/m) coincides very well with the region of minimum plasma density (< $10^4/cm^3$). In the discussion section we will explore the importance of the anticorrelation of the plasma density and the electric field.

Figure 9*b* shows the corresponding electron and ion temperatures with a data gap again occurring within the center of the trough region. The missing temperatures within the trough region are not recoverable, as this information is much more sensitive to a poor signal to noise ratio and spectral distortion than are the line-of-sight velocities. The latitude dependent electron temperature is consistent with the presence of the diffuse aurora at the poleward edge of the trough region at a distance of about +0.4 in our L shell system. The increase of both ion and electron temperatures at the edge of the trough region is observable and is very likely present throughout the trough region. Another feature consistent with other scans of this day and on the April 21 day (refer to Figure 3*b*) is the anticorrelation of the ion and electron temperatures just at the poleward edge of the trough region. We again use a dashed line and note that the temperature determination is not valid in this region [*Swartz et al.*, 1988].

The importance of this specific radar scan lies in the fact that we had a simultaneous HILAT satellite pass and the DMSP F7 satellite pass only 20 min previously. The radar scan sector and the HILAT and DMSP F7 satellite crossings are compared geographically in Figure 10*a*. Due to the close temporal and spatial proximity of the satellite passes with the radar scan, accurate comparisons of various ionospheric properties are possible particularly since the electron and ion particle precipitation data are also available. These can be used as input parameters in the magnetosphere-ionosphere coupling model which may give an accurate and detailed description of trough phenomena.

Electron and ion particle precipitation data from the HILAT and DMSP systems are shown in Figures 10*b* and 10*c*. For comparison purposes, the satellite data are plotted in the same L shell "trough coordinate" system as the radar data (see Figure 9). The DMSP data shows an intense region of ion precipitation shifted equatorward of the electron precipitation by approximately 0.4 in L shell. The ion precipitation boundary lies near the poleward edge of the radar measured plasma trough region. This agrees with the April 21 day in that the ions at the inner edge of the ring current have pushed inward farther than the electrons. The HILAT satellite electron precipitation data were taken within minutes of the radar scan and agree well with radar-measured electron temperatures and densities in determining the edge of the diffuse aurora to be about 0.4 of an L shell (200 km) poleward of the trough center. The difference in the location (≈ 0.5 L shell) of the electron precipitation boundary edge measured by the HILAT and the DMSP satellites may be attributed to a longitudinal undulation of the equatorward edge of the diffuse aurora (see, for example, Plate 2 and *Mendillo et al.* [this issue]).

Figures 11*a* and 11*b* are plots of the ion velocity and the plasma density measured by the HILAT satellite. The satellite velocity measurement had a spatial resolution better than 1 km while the radar resolution was only 35 km. Therefore, we have averaged the HILAT data to 35 km so as to allow comparison with the radar measurements in Figure 11*a*. The figure also shows a plasma density trough at an altitude of 800 km which is coincident with the location of an intense westward velocity. The latter is centered at an L shell of approximately 3.25, which agrees closely with the radar data shown in Plate 2. Since the HILAT satellite had a sine wave-like perturbation in its velocity data due to the spacecraft yaw, we have made a

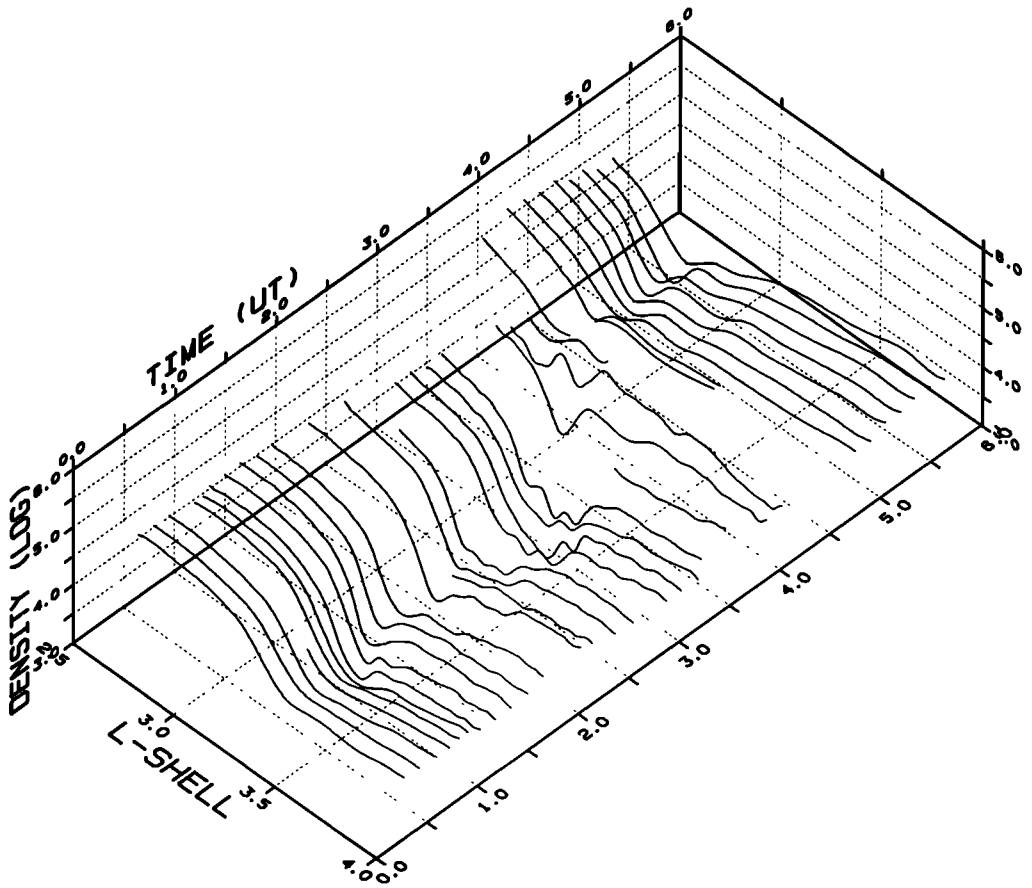

Fig. 6. (*a*) Radar-measured electron density profiles at a fixed altitude of 309 km plotted versus *L* shell and universal time.

sine wave fit to the data in order to generate the velocity plot shown. The short-scale fluctuations in the velocity are therefore more reliable than the absolute or long-period variations plotted here due to possible errors in our substraction of the yaw induced signal. The density trough profiles measured by the radar and HILAT satellite agree well in their latitudinal form in that both measurements show a sharper gradient on the equatorward side than on the poleward side of the trough. There is a tendency for the trough at the height of 800 km to be shifted poleward from the velocity structure. An expanded plot using the full resolution of the HILAT data is given in Figure 11*b*. This shows an extremely structured velocity pattern with several counterstreaming regions of eastward flow. The HILAT satellite electron precipitation instrument recorded an intense (6 ergs/cm^2 s sr), but very soft (≈30 eV) downward electron flux in the region of the horizontal bar which is labeled particle flux). This was the only precipitation recorded in the region equatorward of $L = 3.95$.

Figure 10*c* shows the average energy of the precipitating ions and electrons measured on the two spacecraft (ions were not measured on HILAT). Notice the extremely steep gradients in ion energy. We are not sure why the ion fluxes show a double peak in spatial location on this particular pass, but the sharp poleward gradient seen here at $\Delta L = +0.7$ has been seen on many other passes (D. Hardy, personal communication, 1987). It is possible the equatorward burst of energetic ions is a detached ion aurora analogous to the detached electron auroral arcs discussed by *Mendillo et al.* [this issue].

Discussion

Magnetosphere-Ionosphere Coupling in the Trough Region

An electric field pointing away from the Earth at several Earth radii at the equatorial plane will map to the ionosphere as a poleward directed electric field which can be observed by both radars and low-altitude satellites. The model put forth by *Southwood* [1977] and *Southwood and Wolf* [1978] provides one explanation for the source of such a field at subauroral *L* shells. Their model suggests that a zonal pressure gradient develops in response to enhanced convection. This pressure gradient then drives a zonally westward flow. In this classic MHD generator the flow velocity V and its electric field are related by $\mathbf{E} = -\mathbf{V} \times \mathbf{B}$. In the model the intensity of this field is inversely proportional to the separation of the ion and electron precipitation boundaries. In order to generate large fields the ion and electron boundary separation (ΔL) must be small ($\Delta L < 0.5$). From Figures 4 and 10 an *L* shell separation (ΔL) between the ion and electron precipitation of about ≈ 0.3 to 0.6 is indicated by our data set.

We note from Figures 4 and 10 that there exists a large ion temperature gradient in the trough region, a feature

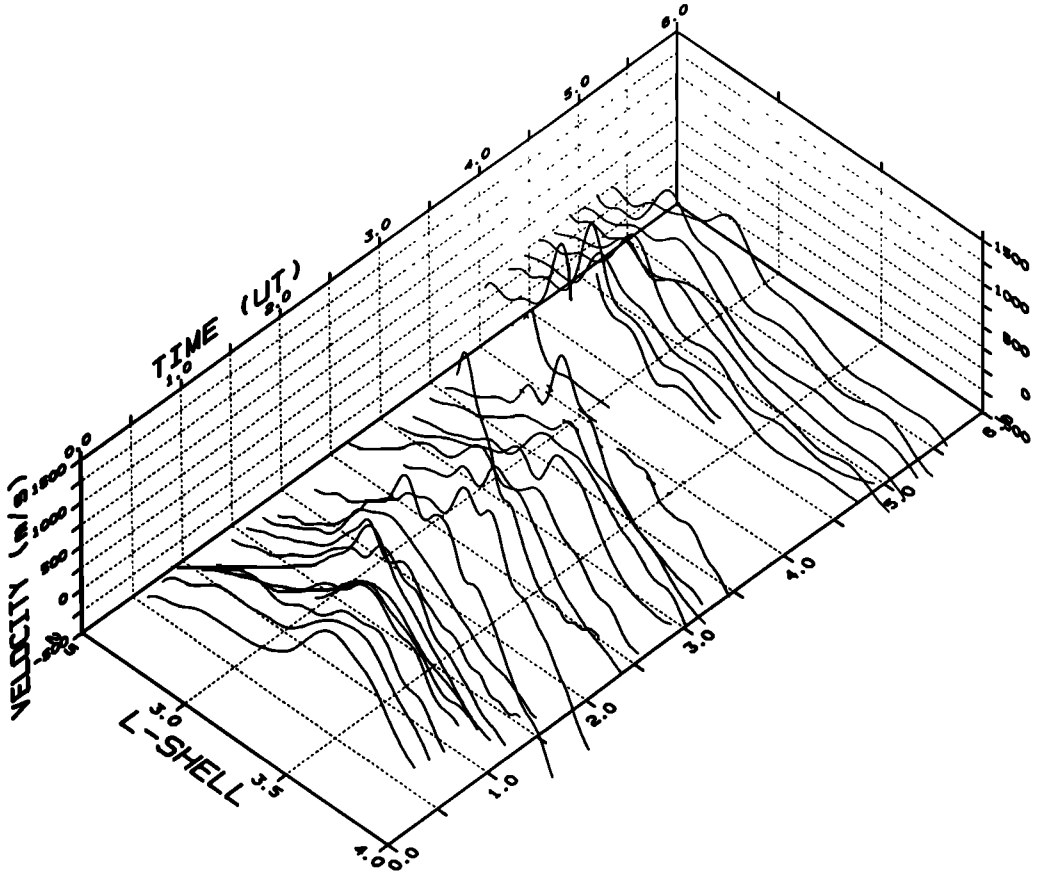

Fig. 6. (*b*) Radar-measured ion drift velocity (assumed to be only zonal) at a fixed altitude of 309 km plotted versus L shell and universal time. Positive is westward, and negative is eastward.

which has not until recently been considered as being associated with large localized electric fields. It has been suggested that the electric field is due to a thermoelectric generator driven by ∇T_i (C. E. Seyler, private communication, 1988). If one assumes the origin of the electric field is due to an ion temperature gradient instead of the usual MHD relation ($\mathbf{E} = \mathbf{U} \times \mathbf{B}$), then $\mathbf{E} = [k_B/e]\nabla T_i$ (C. E. Seyler, private communication, 1988). The average ion energy measured by the DMSP satellite for the April 20 and 21 days (Figures 4*b* and 11*b* respectively) clearly indicates a temperature gradient in the direction of the measured electric field at the poleward edge of the plasma density trough region. The April 20 ion data give an equivalent peak antiearthward electric field near the equatorial plane of ≈ 5 mV/m while the pass on April 21 indicates about a ≈ 9 mV/m field. *Maynard et al.* [1980] have reported similar strengths of in situ measurements of electric fields by the ISEE 1 satellite. An important point to note is that the electron precipitation poleward of the ion precipitation produces a high E region conductivity which will short out a localized magnetospheric electric field. The two boundaries that define the location of the large electric field are the inner edge of the ring current and the ring current itself. We have assumed that the satellite-measured ion precipitation originates from the inner edge of the ring current and the electron precipitation originates from within the ring current. In either explanation, the separation of the ring current ions and the plasma sheet electrons does seem to play an important role in the formation of these large electric fields.

The existence of a large ∇T_i may suggest that east-west flows in the equatorial plane of the magnetosphere need not be given by the local $\mathbf{E} \times \mathbf{B}$ drift since there is a large contribution from the ion diamagnetic drift (a two-fluid contribution). This would not be true for the MHD generator. Pure ionospheric measurements cannot unambiguously distinguish between these two mechanisms. Simultaneous measurements of the electric field and the ring current plasma flow are required. In either mechanism the ionospheric conductivity and closure current in the magnetosphere are important parameters, and in the next paragraphs we use the present data set to estimate these quantities.

In order to understand how such large electric fields may be sustained for periods of 30 to 90 min at a time, it is important to examine the height-integrated Pedersen conductivity Σp in the ionosphere. In the daytime and in the auroral ionosphere the conductivity is dominated by the E region. However, vertical density profiles we have taken with the Millstone Hill radar on April 20 and which were presented in Figure 8 show that the nighttime mid-latitude F region contains the bulk of the Pedersen conductivity. This result agrees with the results of an extensive study of the E region and F region height-integrated conductivities using the Arecibo Observatory [*Burnside et al.*, 1983]. Burnside et al. showed that the F region Pedersen

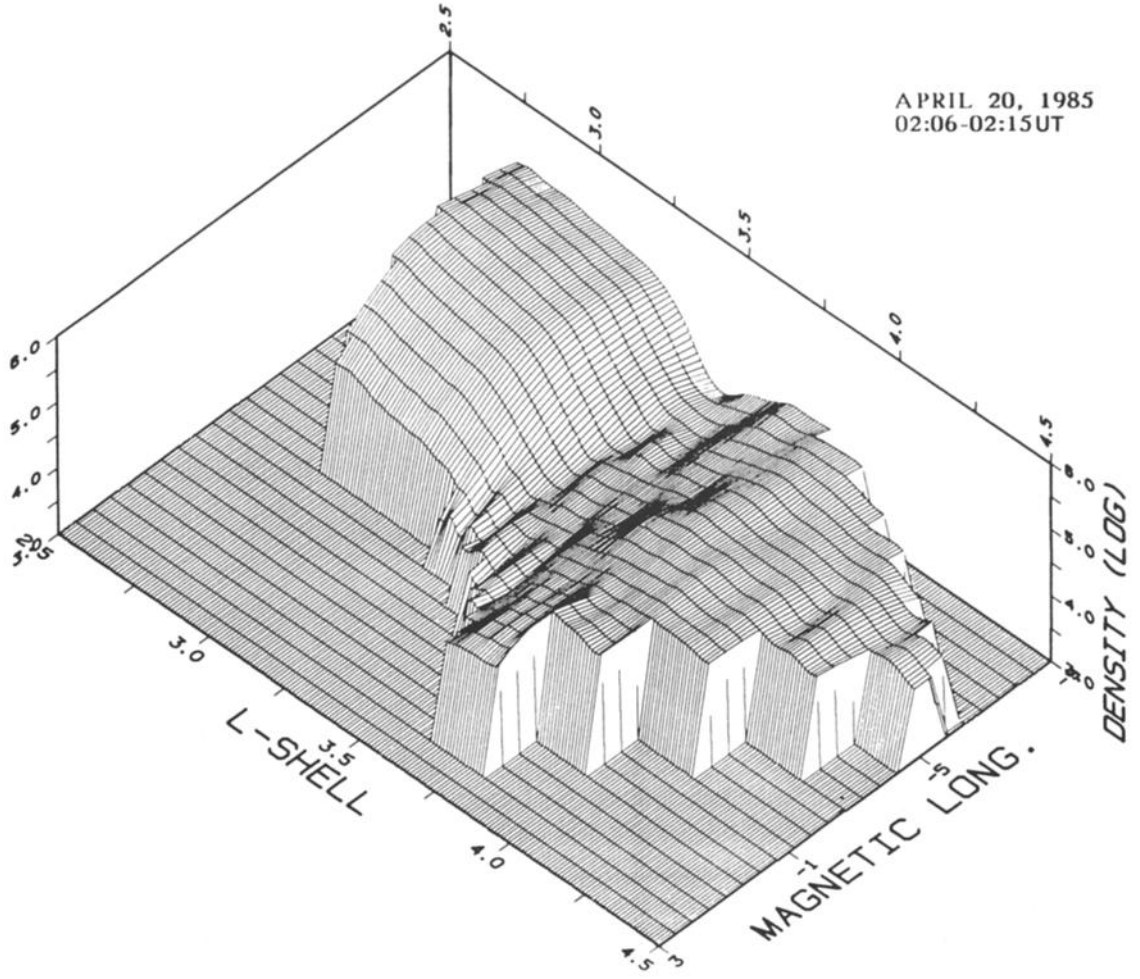

Fig. 7. Electron density profile scan plotted on a logarithmic scale versus magnetic coordinates. The plot covers an altitude of 187-488 km.

conductivity was on average 10 times larger than *E* region Pedersen conductivity at night. The ratio was dependent upon season and local time but was seldom less than unity. The mid-latitude *F* region therefore plays a dominant role at night in determining the height-integrated conductivity, and so any nonuniform conductivity in this region will have a large impact on the field-aligned currents. In the study of large subauroral electric fields carried out by *Banks and Yasuhara* [1978], only the *E* region conductivity was considered. In the work reported here we include the dominant contribution of the *F* region and come to the same conclusions as *Banks and Yasuhara* [1978] but for a different reason: the current required to maintain the electric field is very small.

To determine the component of the current density parallel to the magnetic field ($J_{\parallel}$), we start from $\nabla \cdot \mathbf{J}$ where $\mathbf{J}_{\perp} = \sigma \cdot \mathbf{E}$. We ignore zonal derivatives to a first approximation and consider only the component of **E** perpendicular to the *L* shell (E_x). Then the Hall term vanishes and one obtains

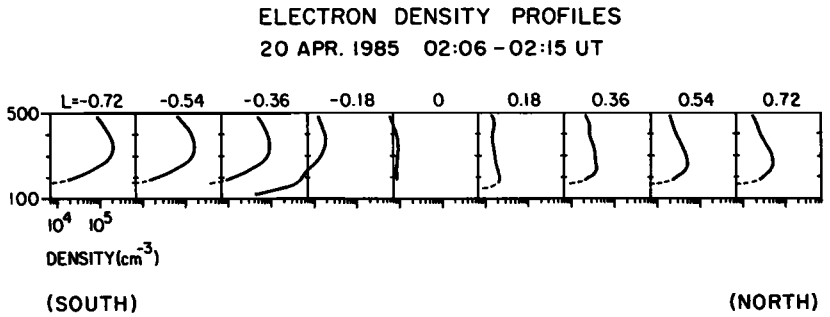

Fig. 8. A cross-sectional cut through the trough region in a north-south direction showing the electron density profile versus altitude. The extrapolation for the *E* region density is represented by a dashed line.

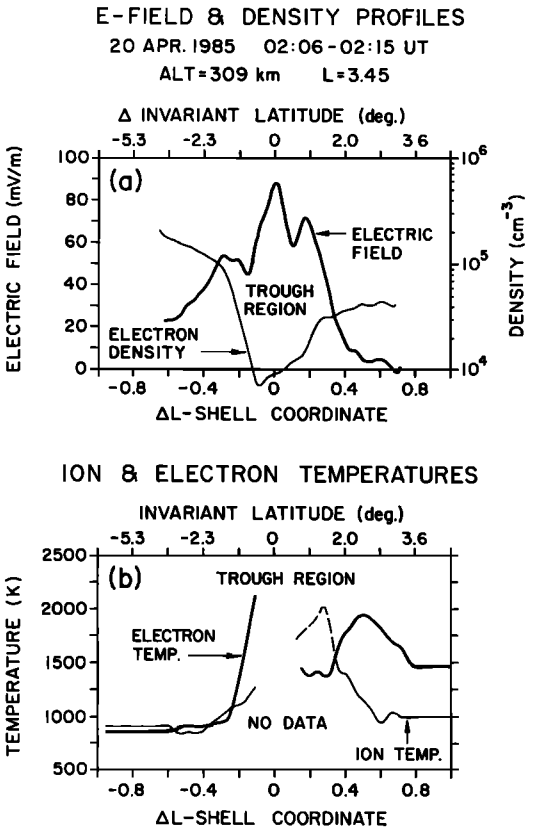

Fig. 9. (*a*) Millstone Hill radar-measured electric field and electron density profiles at an altitude of 309 km. (*b*) Corresponding electron and ion temperature profiles. The radar analysis program indicated that electron and ion temperatures have an accuracy of better than 5% for $|\Delta L| > 0.3$ and 10% for $|\Delta L| < 0.3$. Both figures use an L shell aligned trough coordinate system.

$$-J_{\parallel} = \Sigma_{\pi} \frac{\partial E_x}{\partial x} + E_x \frac{\partial \Sigma_p}{\partial x} \qquad (1)$$

Under these same approximations, we use $\nabla \times \mathbf{B} = \mu_0 \mathbf{J}$ to calculate the perturbation magnetic field due to this current,

$$\delta B_{\perp} = \mu_0 \Sigma_p E_x + \text{const} \qquad (2)$$

Equation (2) holds if the measurement of $\delta B_{\perp}$ is made high enough above the ionosphere that it is only due to the field-aligned current. Often in high-latitude applications, the spatial variation in the height-integrated Pedersen conductivity (Σ_p) is assumed constant, and therefore the second term in equation (1) is neglected. However, as we shall see within the trough region, this assumption is incorrect.

For this study we concentrate upon the scan which was closest in time to the HILAT pass since magnetic field measurements are available on the satellite. Our best estimate of $\Sigma_p(x)$ is plotted in Figure 12*c*. The F region value is obtained directly from the Millstone Hill data. We have added a constant value of 0.15 mho for the E region contribution which is typical for a mid-latitude, nighttime E region. In addition, we include a sharp increase in Σ_p obtained by a calculation based upon the precipitating electron fluxes measured by HILAT (J. Vickrey, personal communication, 1987). We have interpolated between the end of the radar Σ_p and the beginning of the HILAT Σ_p. A polynomial was matched to the electric field data as shown in Figure 12*b*. For reference the associated potential is also plotted as a function of x, assigning 0 volts to the equatorward edge of the region. The total potential is 30 kV, a number quite similar to the potentials found by *Rich et al.* [1980], who studied seven such events. The field-aligned current calculated from equation (1) is plotted in Figure 12*a*. Extremely small currents are predicted, less than 0.04 μA/m².

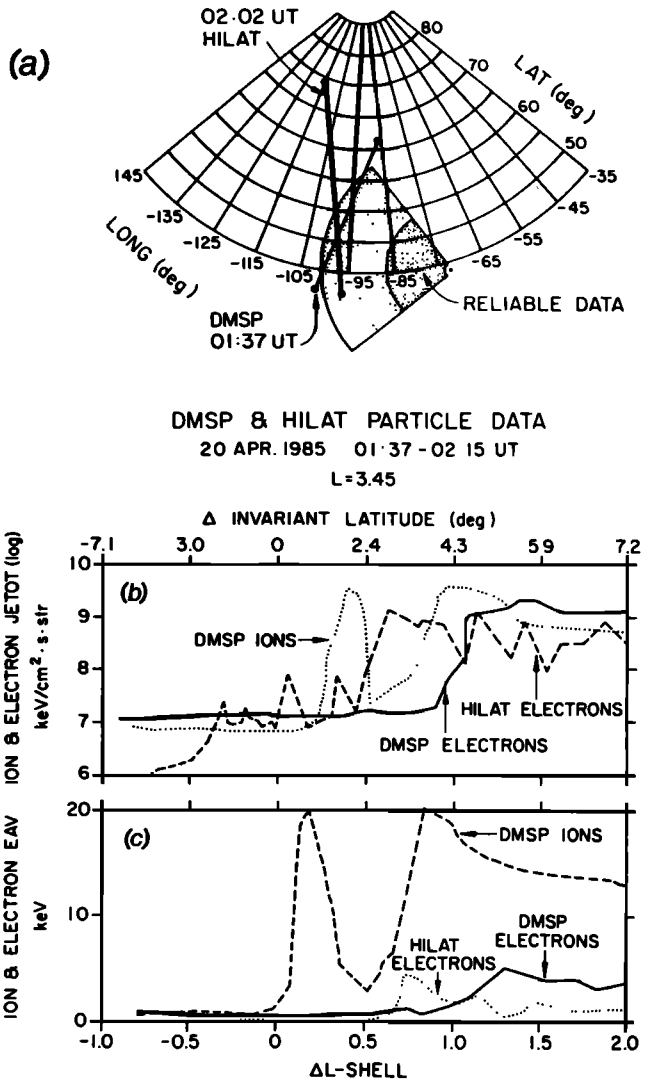

Fig. 10. (*a*) Plot of the HILAT and DMSP satellite trajectories in geophysical coordinates coincident with the radar scan on April 20, 1985. (*b*) Total ion and electron energy flux. (*c*) Electron and ion average energy. Figures 10*b* and 10*c* use the same L shell (invariant latitude) trough coordinate system centered at $L = 3.45$. A significant change in the DMSP ion total flux and average energy occurred between $\Delta L = 0.0$ and 0.5 and between $\Delta L = 0.5$ and 0.8. A significant change in the DMSP electron total flux and average energy occurred between $\Delta L = 0.8$ and 1.3. The HILAT satellite electron average energy and total flux curves show a significant change between $\Delta L = 0.0$ and 0.5 (soft particle precipitation) and between $\Delta L = 0.5$ and 0.7 (energetic particle precipitation).

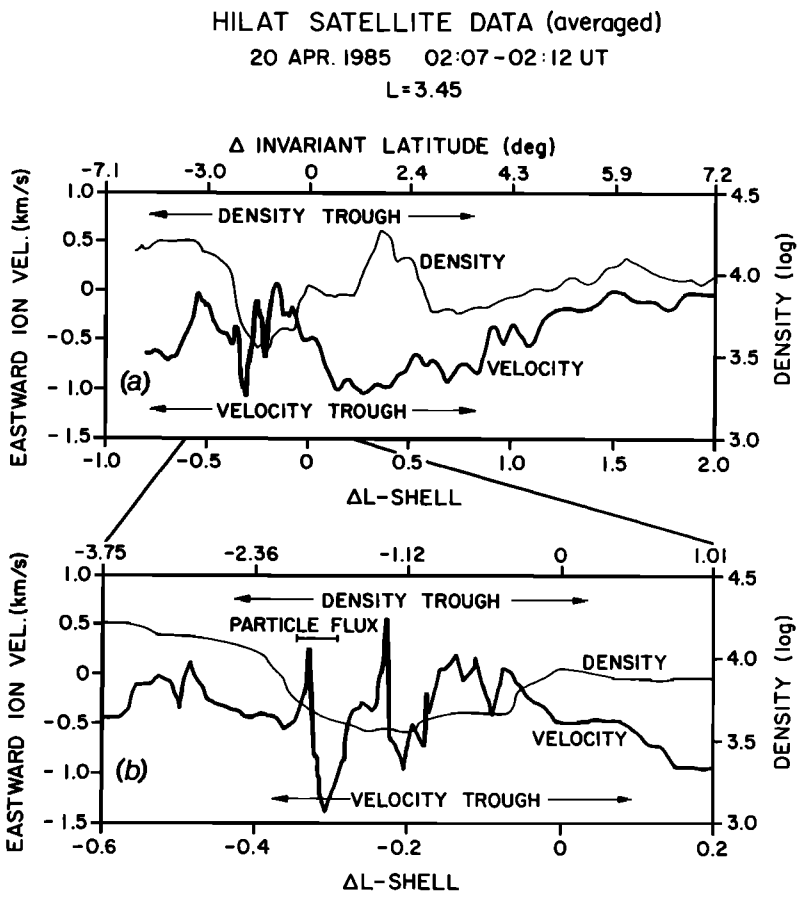

Fig. 11. (*a*) The HILAT satellite-measured density and ion velocity averaged to a resolution of 35 km versus an L shell (invariant latitude) aligned trough coordinate system centered at $L = 3.45$. (*b*) The same data versus an expanded L shell (invariant latitude) aligned trough coordinate system.

A similar electric field pattern in the auroral oval would be associated with currents 3 orders of magnitude higher. The importance of structure in the F-region can be seen from the thick curve in Figure 12*a*. Here we have plotted the field-aligned current which would arise in an unstructured mid-latitude ionosphere with $\Sigma_p = 0.55$ mho. Two current sheets arise with $J_\parallel \approx 0.16$ μA/m, 4 times larger than the value including the $\Sigma_p(x)$ variation.

To compare these calculations with the experiment data, we have used equation (2) to calculate the predicted magnetic field (setting the integration constant equal to zero) and plotted this on the same scale as the measured magnetic field in the trough region in Figure 12*d*. The magnetic signal detected by HILAT was so small that it is buried in the noise level of the instrument. It is clear, however, that δB is very small and, if anything, that the value we have calculated overestimates the measured value. For reference the peak magnetic perturbation predicted for an undisturbed $\Sigma_p(x)$ is 50 nT, clearly much larger than found by the HILAT instrumentation.

These results point out the importance of the F region trough in controlling the load imposed upon the magnetospheric generator. *Banks and Yasuhara* [1978] emphasized the role of the E region and pointed out that the compressibility of the latter would lead to a $\Sigma_p(x)$ which lowers the required $J_{||}$. A feedback occurs in their case since the large applied E field creates the change in $\Sigma_p(x)$. Our results show the F region to be the controlling factor, but we come to a similar conclusion. That is, since our impressed electric field results in a deep ionosphere F region trough (see the next section), the ionospheric load on the generator decreases drastically as the ionospheric plasma becomes structured. Since Figure 8 (L = -0.18) shows the measured E region density to be less than 800 cm^{-3}, it could well be that the image mechanism proposed by *Banks and Yasuhara* [1978] is also operating in the E region. This effect would further reduce $J_\parallel$, and hence $\delta B_\perp$ would be in even better agreement with the HILAT signal.

Given that we know Σ_p and E_x, it is possible to calculate the power (watts per meter) dissipated per unit length in the ionospheric trough region using the following relationship:

$$P_i = \int [\Sigma_p E_x] E_x \, dx \ \text{W/m} \qquad (3)$$

Evaluating the above relation gives $P_i \approx 400$ W/m. Since this power must be supplied from the generator, we can estimate the power density supplied from the magnetosphere. In a dipole field, *Mozer* [1970] showed that the azimuthal separation between two field lines spreads as $2L(L\text{-}3/4)$ which yields a factor of 12 for L=3.5. Since there are two ionospheric loads, the power per unit length in the equatorial plane (P_m) should be ≈ 70 W/m. In the equatorial plane, P_m is expressed as follows;

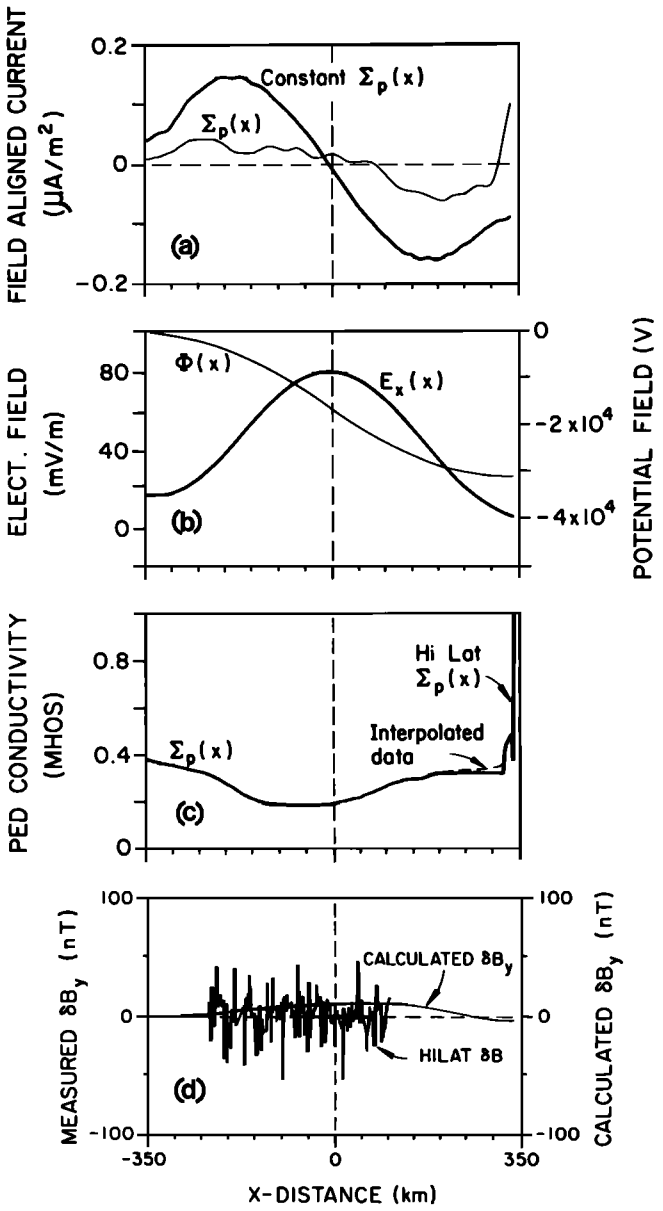

Fig. 12. (*a*) Comparison of the calculated field-aligned current using the electric field and conductivity profiles shown in Figures 12*b* and 12*c* with a calculated $J_{\parallel}$ using the same electric field profile but a constant conductivity profile of 0.55 mho. (*b*) Fifth-order polynomial fit to the measured electric field profile of April 20, 1985, shown in Figure 7. (*c*) Calculated Pedersen conductivity ($\Sigma_p(x)$) derived from the Millstone Hill radar-measured electron density and the HILAT satellite-measured precipitating electron fluxes. (*d*) The calculated δB_y and the HILAT satellite measured δB_y versus horizontal distance.

$$P_m = \int [\mathbf{J}_m \cdot \mathbf{E}_m]\, dr\, dz \quad \text{W/m} \tag{4}$$

where $\mathbf{J}_m$ is the radial directed current density (amperes per square meter) and $\mathbf{E}_m$ is the radial directed electric field in the equatorial plane with the r representing the radial direction and z representing vertical direction (parallel to B). In the generator, $\mathbf{J}_m \cdot \mathbf{E}_m$ must be negative in order to supply energy to the ionosphere. To proceed we will assume that the current density $\mathbf{J}_m$ has the same radial dependence as the electric field and that both have a Gaussian dependence upon r. We further assume that the generator occupies less than 10% of the field line length in the z direction (parallel to B), and we then are able to estimate $\mathbf{J}_m$. Figure 12*b* shows that the Gaussian form $\exp\{-r^2/a^2\}$ is characterized by a = 2000 km, and the minimum vertical extent is estimated to be about 3000 km. After evaluating equation (4), and setting it equal to 70 W/m we find the maximum value of $\mathbf{J}_m \approx 1.2 \times 10^{-4}$ mA/m^2.

The east-west pressure gradient needed to generate such a $\mathbf{J}_m$ is given by $\nabla p = \mathbf{J}_m \times \mathbf{B}_m$ where $\mathbf{B}_m$ is taken at the equatorial plane (≈ 0.007 G). We find ∇p to be about 8.5 x 10^{-17} J/m^4. For a 10-keV plasma with a density of 1 cm^{-3}, this pressure gradient corresponds to a gradient scale length in the azimuthal direction of ≈ 3 R_e with a direction pointing from dusk to midnight. The perturbed magnetic field in this region would be directed toward midnight and be of the order of 1.2×10^{-7} nT. Such a pressure gradient is consistent in magnitude and direction with either the *Southwood and Wolf* [1978] or the thermoelectric generator mechanism. The key observable difference is the velocity perturbation in the equatorial plane. In the former case, a region of intense flow roughly 1 R_e wide should be detected with peak value in excess of 50 km/s. In the latter case the net ion flow velocity should be less since the $\mathbf{E} \times \mathbf{B}$ drift is opposed by an eastward drift due to the radial ion pressure gradient.

Effects of the large Electric Field Coupling on the Ionosphere Trough

In the data set described here we have examples where the position of the region of high plasma flow velocity leaps equatorward in seeming response to changing magnetospheric conditions (e.g. as indicated by *Dst* variations). The localized high-flow region in the thermosphere subsequently exhibits development of a deep colocated plasma density depletion. The rapid formation of a deep plasma density trough thus seems to be a direct consequence of an intense and localized electric field. The electric field is generated at the inner edge of the ring current for reasons discussed above and maps to the ionosphere. To fully understand the time evolution of this density trough requires a model that incorporates not only electric field dependent chemical reactions but also electrodynamical transport processes which we review in the next paragraphs.

Schunk et al. [1975] have shown that a large increase in the O^+ loss rate can be associated with large ionospheric electric fields. Both high ion temperatures and substantial ion flow speeds play a role in this process. They developed a model in which a strong electric field can play the dominant role in the formation of a colocated F region plasma density trough. In their paper, they show there is a strong dependence of the reaction rate on an applied electric field for the process of $O^+ + N_2 \rightarrow NO^+ + N$. The reaction coefficient is temperature dependent as well as dependent on the velocity difference between the neutral and ion particles. Both factors are strongly influenced by the strength of the perpendicular electric field.

The present data set allows the evolutionary behavior of the trough to be studied for the first time. We consider first the question of how the trough position and shape depend on the position and intensity of the poleward directed electric field. Figures 6*a* and 6*b* indicate that the radar observations are in general agreement with an anticorrelation between the plasma density and the applied poleward directed electric field. However, our data indicate the rate of plasma depletion is much greater than that predicted by the model. For example, *Schunk et al.* [1976] predict that if there is no net upward plasma flux, a starting density of 3.8×10^4 cm^{-3} only evolves to a plasma density of 1.8×10^4 cm^{-3} after an effective electric field ($E_\perp'$) of 50 mV/m has been applied to the ionosphere for a period of 1 hour. The effective electric field includes a term due to the neutral wind, U_n,

$$\mathbf{E}_\perp' = \mathbf{E}_\perp + (\mathbf{U}_n \times \mathbf{B}) \quad (5)$$

A north-south electric field of 60 mV/m is required in order to have an effective electric field of 50 mV/m, if a westward neutral wind of say 200 m/s exists in the same direction as the ions. The radar data indicate that 60-mV/m electric fields are easily present within the storm time trough region and can be maintained for periods of 1 hour.

Figure 13 is a plot versus time of relative density (N) normalized to an initial peak plasma density (N_{max}) of 3.8×10^4 cm^{-3} that shows both measured and predicted rates of the plasma depletion in the trough region. The data plotted correspond to two different time periods on April 20. The first data set was taken between 0019 UT and 0045 UT. The five points plotted correspond to an altitude of 309 km, located on an L shell of 3.5. The second data set was taken between 0254 UT and 0334 UT with the three points plotted corresponding to an altitude of 309 km at an L shell of 3.1. The two plots of predicted plasma density decay are from *Schunk et al.* [1976] for the case of zero upward flux of plasma and for the case where upward flux was assumed to be initially 1.8×10^8 cm^{-2} s^{-1} and is assumed to be proportional to $N(O^+)^{5/8}\ T_i^{3/2}$ [*Geisler*, 1967]. It is

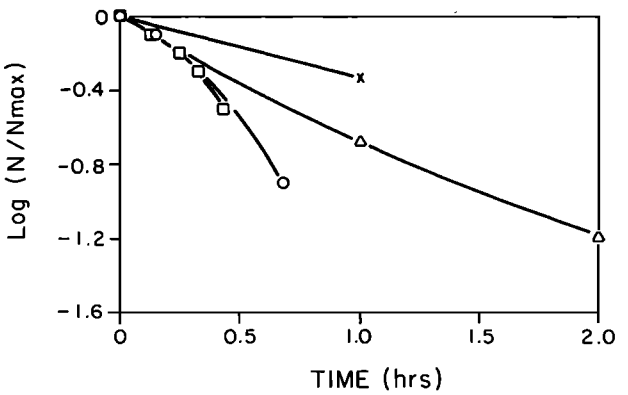

Fig. 13. Plot of the ratio of electron density (N) at the F peak to the initial electron density (N_{max}) versus time: (cross) model data points, $N_{max} = 3.8 \times 10^4$ cm^{-3}, upward flux = 0.0; (triangle) model data points, $N_{max} = 3.8 \times 10^4$ cm^{-3}, upward flux (t=0) = 1.8×10^8 cm^{-2} s$^{-1} \sim N(O^+)^{5/8} T_i^{3/2}$; (square) radar data points, $N_{max} = 3.2 \times 10^4$ cm^{-3}, time = 0019-0045 UT, $L = 3.5$; and (circle) radar data points, $N_{max} = 3.1 \times 10^4$ cm^3, time = 0254-0334 UT, $L = 3.1$.

apparent that the data show the rate of plasma decay which is much larger than predicted by the model. A relationship between the upward flux and the electric field intensity can be seen in data from the AE-C satellite described by *Spiro et al.* [1978]. In their data set, one can clearly see a correlation between a rapid westward ion drift spike and an increase in the upward flux of thermal plasma. The upward velocity was in the range 250-300 m/s. Since the measured density at the same height was 10^3 cm^{-3}, such a flow corresponds to a flux of 2.5×10^7 to 3.0×10^7 cm^{-2} s^{-1}. This flow value is somewhat less than that used by *Schunk et al.* [1976], however, and is therefore not sufficient to explain the rapidity of trough development.

Another explanation for a rapid trough depletion involves advection of a lower-density plasma from a position east of the observatory point. The high westward flow velocity tends to amplify the importance of such a gradient ,and we can estimate the latter as follows. From Figure 13 the e-folding time τ seems to display two characteristics. Initially the Schunk model (with outflow) seems to be followed with $\tau = 15$ min. After roughly 20 min have passed, τ increases to a value closer to 40 min. Our measurements show that τ continues to be approximately 15 min. Assuming that advection dominates, we have

$$\frac{\partial n}{\partial t} = -(\mathbf{V} \cdot \nabla) n \quad (6)$$

Assuming $n = n_0 \exp\{-t/\tau\}$ with $\tau = 15$ min and $v = 1000$ m/s yields

$$L = (10^3 \text{ m/s})\ (900 \text{ m/s}) = 900 \text{ km}$$

That is, if a westward directed plasma density gradient exists with an e-folding length of 900 km, the local density could decrease at the rate observed. At the observation latitude this distance corresponds to about 1 hour of local time. Although we cannot present direct evidence that this occurs nor even make a plausible argument that such a gradient exists, we cannot rule out this explanation as a source for the observed rapid local depletion time scale, and it certainly bears further study.

Figure 14 shows a number of two-dimensional plots of the same velocity and plasma density profiles shown in Figures 6*a* and 6*b* which depict how both the electric field and plasma trough evolve in time. The lines drawn in Figure 14 show that trough formation appears to lag behind the movement of the electric field. The lag is most noticeable in the time periods between 01:13 and 02:48 UT and can be as great as 0.3 L shell. As the electric field moves poleward it cuts a deep depletion in the F region, causing the trough to broaden in latitude. The plasma density equatorward of the broadened trough stays relatively unchanged from a typical nighttime density profile.

The initial ion and electron density profiles ($t = 0$) used by *Schunk et al.* [1976] correspond to the daytime mid-latitude profiles calculated by *Schunk et al.* [1975]. These ion and electron profiles seem reasonable in regions equatorward of the trough. However, we see from Figure 6 that the plasma density profiles poleward of the trough are much different. The plasma density profiles we find in the

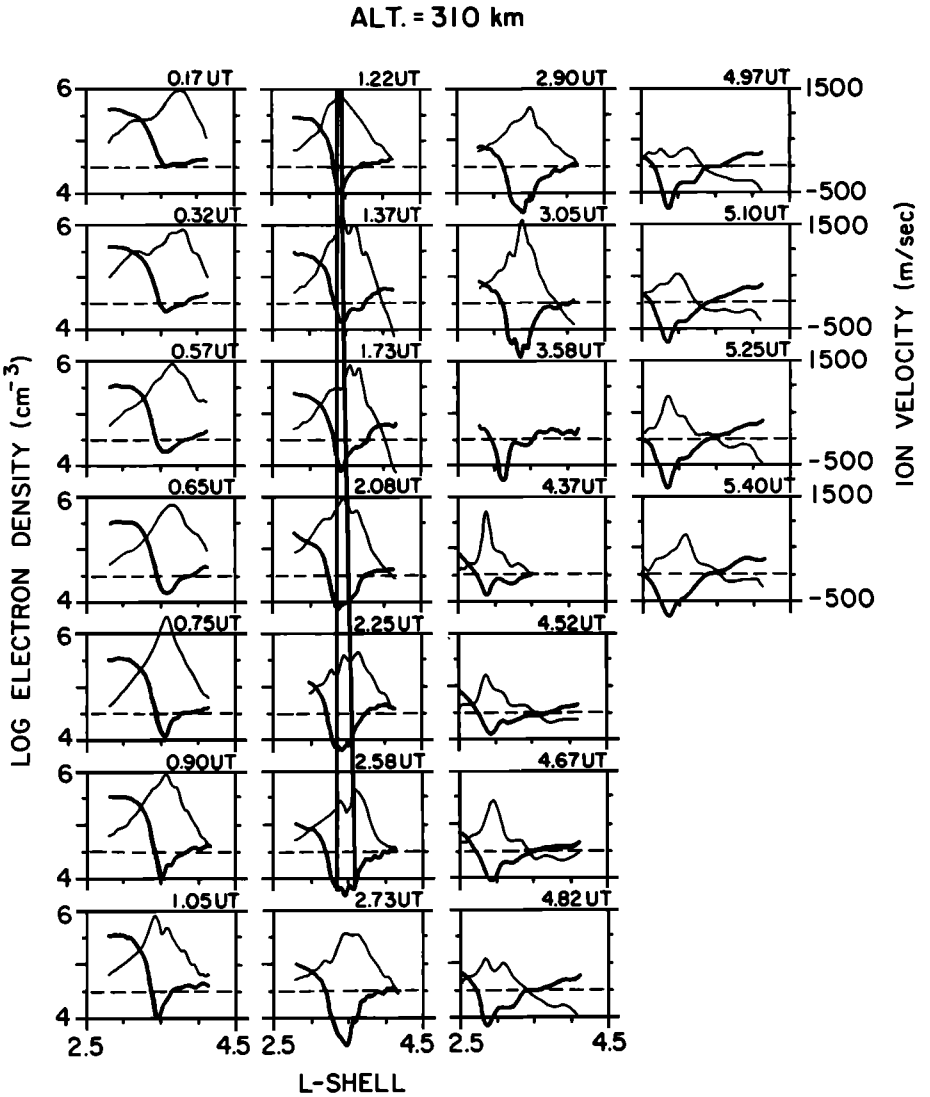

Fig. 14. Plot of the electron density and the plasma velocity versus L shell. The plasma velocity is calculated assuming only a pure zonal direction. Positive velocities correspond to westward directed flows. The approximate locations of the electron density minima and ion velocity maxima are shown in the center column of panels by a thick and a thin line, respectively. These two lines show that the electron density minima can lag behind the velocity maxima during periods of rapid trough movement.

poleward zone have the F region peak at a much lower altitude (< 250 km) and an increased plasma scale height (elevated electron temperatures). Future trough models may have to assume different density profiles across the trough region in order to explain the rapid development we report here.

On the Undulation of the Edge of the Diffuse Aurora

In the companion paper by *Mendillo et al.* [this issue], it is shown quantitatively that the undulations in 6300 Å mirror a similar structure in the precipitating particles. This correspondence was clear in the study by *Lui et al.* [1982] since the DMSP observations were made in the 3914-Å band. For 6300 Å, *Mendillo et al.* [this issue] have shown in addition that the observations were not due to emissions associated with the recombination of O^+ and hence not due to a structuring process local to the ionosphere. Of course, this result does not imply that the local ionosphere is smooth since the precipitation of the electrons is a primary source of the ionization poleward of the trough.

Comparison between HILAT and DMSP (F7) particle fluxes and both sets of ground data shows the various boundaries are not perfectly L shell-aligned. For example, Figure 12*a* shows the HILAT and DMSP measurements of electron flux. The equatorward boundary of the electron flux corresponds to the equatorward edge of the diffuse aurora. The radar data (see Figure 10) agree with HILAT electron precipitation in determining the location of the equatorward edge of the diffuse aurora ($L \approx 4$). However, the DMSP measurements show that the electron precipitation boundary lies at an L shell of about 4.5. This suggests that an undulation does exist along the poleward edge of the trough. The radar data by alone are ambiguous since it is difficult to distinguish between longitudinal and altitude variations in the scanning data. On the following day (April 21), both the radar and the optical measurements

(see Figure 3) show clear undulations along the poleward edge of the trough.

Turning to the origin of these undulations, the optical data seem to favor some type of interchange instability since no evidence exists for a high phase velocity of the structure along the edge of the diffuse aurora. For example, this seems to rule out the suggestion by *Kelley* [1986] that a Kelvin-Helmholtz instability [*Vinas and Madden*, 1986] should be driven by a high shear in the plasma flow. Care must be taken in this regard, however, since the electron precipitation is by definition located in a region of high ionospheric conductivity which is just poleward of the high-shear region. If surface waves are generated and penetrate into the slow flow velocity region where the hot electrons are located, the apparent phase velocity might be quite low. An interchange instability driven by an electric field due to field line curvature was considered by *Vinas and Madden* [1986], as was a ballooning instability which also has a slow phase velocity.

CONCLUSIONS

For the first time both incoherent radar and satellite instruments have made simultaneous measurements of large westward plasma drifts (> 1500 m/s) located near the equatorward edge of the diffuse aurora. These intense localized electric fields occurred during a magnetic storm as evidenced by the *Dst* index. There is some evidence for a shift of the latitude of the large electric field region when the ring current intensified. Plots of the radar-measured plasma density profiles in a magnetic coordinate system show that the zero-order structure of the trough region is L shell aligned to first order. Latitude dependent electron temperatures and plasma density show the presence of the diffuse aurora at the poleward edge of the trough region. The optical measurements, satellite measurements, and radar density scans are in good agreement in the determination of the trough region. Longitudinal undulations can be seen in the above sets of observations. Comparison between optical, radar, and satellite data shows that undulations are a magnetospheric phenomenon in which the electron precipitation itself is spatially modulated. This in turn creates the modulations in light emissions and plasma density. On April 21 and April 20 the diffuse aurora ends approximately at 0.8 and 0.4 of an L shell poleward of the trough region, respectively.

Since we could track the development of the trough, a comparison with theory is possible. We find a much more rapid trough depletion rate than predicted, even taking into account a high plasma outflow velocity. We suggest that either rapid plasma heating and subsequent redistribution of plasma with height or advection of a lower-density region from a later local time may explain this discrepancy.

The radar data show the electric field and F layer plasma density are anticorrelated and that most of the conductivity is in the F region. This implies that the horizontal current is nearly divergence free and that the parallel currents from the magnetosphere required to support the large electric field are small, less than 0.04 $\mu A/m^2$. This result is in good agreement with the HILAT magnetometer data which showed very small field-aligned currents.

The satellite measurements of the ion precipitation at the poleward side of the trough show a temperature gradient in the direction of the measured electric field. This suggests the intriguing possibility that the electric field is due to a thermoelectric generator driven by ∇T_i.

APPENDIX

Since it is generally accepted that large-scale electric fields map from the magnetosphere to the ionosphere, it is important in the determination of a trough coordinate system to investigate the electric field profile derived from observed line-of-sight ion velocities. At this point, it is important to discuss how these velocities were generated. Millstone Hill applies a mean square estimation technique in determining the line-of-sight ion velocities (i.e., the new Doppler shift in frequency of the spectra) which is very accurate for those spectra that have good S/N (signal to noise ratio) and minimum variation from the expected shape of the spectra. Unfortunately, as the radar beam approached the region of low plasma density, the S/N ratio became poor and, in addition, some of the spectra were corrupted by either coherent echoes from E region instabilities or velocity shears within the scattering volume. The poor S/N and unusual spectra caused the Millstone Hill analysis program to fail. Examination of each spectrum (excluding those corrupted by coherent echoes) for which the Millstone Hill program failed suggests that one could still take the first moment of the spectrum to get an approximate value of the ion line-of-sight drift velocities.

A correction to the measured line-of-sight velocities was made by assuming the primary flow of ions was zonal. The radar line-of-sight vector was computed for each data point in the magnetic field coordinate system, and then the angles were computed as shown in Figure A1. Given the angles ϕ and θ, we then calculate the E-W (zonal) velocity component. The final step was to smooth the data using a cubic spline approximation technique.

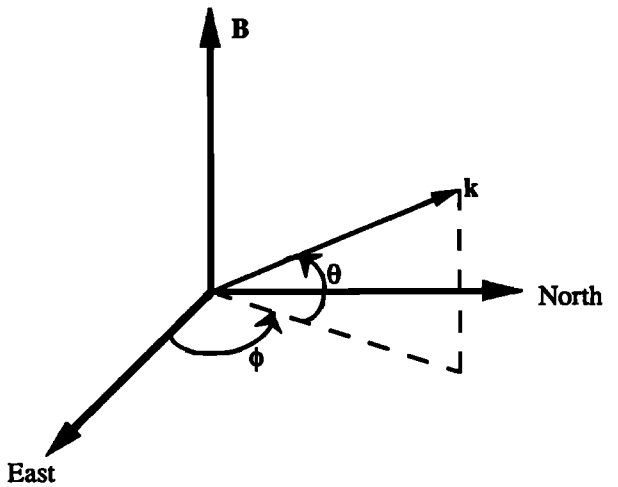

Fig. A1. Magnetic field coordinate system for the radar line-of-sight vector.

Acknowledgments. We acknowledge useful discussions with Jason Providakes and C. E. Seyler. We thank the staff of Millstone Hill incoherent scatter radar observatory for assisting in the radar observations which were supported by NSF cooperative agreement ATM-84-19117. We are grateful to B. Livingston and J. Vickrey for their valuable assistance with the HILAT satellite data. The DMSP satellite data were kindly provided by D. Hardy and N. Heinemann. We also thank L. Lanzerotti for his assistance in the magnetometer observations. This work was supported by the Atmospheric Sciences Division, National Science Foundation, under NSF grant ATM-85-11811 at Cornell University.

The Editor thanks F. Creutzberg and A. Rodger for their assistance in evaluating this paper.

REFERENCES

Banks, P. M., and F. Yasuhara, Electric fields and conductivity in the nighttime *E* region: A new magnetospheric-ionosphere-atmosphere coupling effect, *Geophys. Res. Lett., 5*, 1047, 1978.

Burnside, R. G., J. C. G. Walker, R. A. Behnke, and C. A. Gonzales, Polarization electric fields in the nighttime *F* layer at Arecibo, *J. Geophys. Res., 88*, 6259, 1983.

Geisler, J. E., On the limiting daytime flux of ionization into the protonosphere, *J. Geophys. Res., 72*, 81, 1967.

Gussenhoven, M. S.,D. A. Hardy, and N. Heinemann, The equatorward boundary of auroral ion precipitation, *J. Geophys. Res., 92*, 3273, 1987.

Kelley, M. C., Intense sheared flow as the origin of large-scale undulations of the edge of the diffuse aurora, *J. Geophys. Res., 91*, 3225, 1986.

LaBelle, J., R. A. Treumann, W. Baumjohann, G. Haerendel, N. Sckopke, and G. Paschmann, The duskside plasmapause/ring current interface: convection and plasma wave observations, *J. Geophys. Res., 93*, 2573, 1988.

Lui, A. T. Y., C.-I. Meng, and S. Ismail, Large amplitude undulations on the equatorward boundary of the diffuse aurora, *J. Geophys. Res., 87*, 2385, 1982.

Maynard, N. C., On large poleward-directed electric fields at sub-auroral latitudes, *Geophys. Res. Lett., 5*, 617, 1978.

Maynard, N. C., T. L. Aggson, and J. P. Heppner, Magnetospheric observations of large subauroral electric fields, *Geophys. Res. Lett., 7*, 881, 1980.

Mendillo, M., J. B. Baumgardner, and J. Providakes, Ground-based imaging of detached arcs, ripples in the diffuse aurora, and patches of 6300-Å emission, *J. Geophys. Res.*, this issue.

Mozer, F. S., Electric field mapping in the ionosphere at the equatorial plane, *Planet. Space Sci., 18*, 259, 1970.

Rich, F. J., W. J. Burke, M. C. Kelley, and M. Smiddy, Observations of field-aligned currents in association with strong convection electric fields at subauroral latitudes, *J. Geophys. Res., 85*, 2335, 1980.

Rodger, A. S., L. H. Brace, W. R. Hoegy, and J. D. Winningham, The poleward edge of the mid-latitude trough-Its formation, orientation and dynamics, *J. Atmos. Terr. Phys., 48*, 715, 1986.

Schunk, R. W., W. J. Raitt, and P. M. Banks, Effect of electric fields on the daytime high-latitude E and F regions, J. Geophys. Res., 80, 3121, 1975.

Schunk, R. W., P. M. Banks, and W. J. Raitt, Effects of electric fields and other processes upon the nighttime high-latitude *F* layer, *J. Geophys. Res., 81*, 3271, 1976.

Smiddy, M., M. C. Kelley, W. Burke, R. Rich, R. Sagalyn, B. Shuman, R. Hays, and S. Lai, Intense poleward-directed electric fields near the ionospheric projection of the plasmapause, *Geophys. Res. Lett., 4*, 543, 1977.

Southwood, D. J., The role of hot plasma in magnetospheric convection, *J. Geophys. Res., 82*, 5512, 1977.

Southwood, D. J., and R. A. Wolf, An assessment of the role of precipitation in magnetospheric convection, *J. Geophys. Res., 83*, 5227, 1978.

Spiro, R. W., R. A. Heelis, and W. B. Hanson, Rapid subauroral ion drifts observed by Atmospheric Explorer C, *Geophys. Res. Lett., 6*, 657, 1978.

Swartz, W. E., J. F. Providakes, M. C. Kelley, and J. F. Vickrey, The effect of strong velocity shears on incoherent scatter spectra: A new interpretation of unusual high latitude spectra, *Geophys. Res. Lett., 15*, 1341, 1988.

Vinas, A. F., and T. R. Madden, Shear flow-ballooning instability as a possible mechanism for hydromagnetic fluctuations at the plasmapause, *J. Geophys. Res., 91*, 1519, 1986.

J. M. Holt, MIT Haystack Observatory, Westford, MA 01886.

M. C. Kelley, J. F. Providakes, and W. E. Swartz, School of Electrical Engineering, Cornell University, Ithaca, NY 14853.

M. Mendillo, Center for Space Physics, Boston University, 725 Commonwealth Avenue, Boston, MA 02215.

(Received February 3, 1988;
revised August 18, 1988;
accepted September 21, 1988.)